Quantitative Modeling of Nucleosome Unwrapping from **Both Ends**

D. Zhao¹, J.V. Le¹, M.A. Darcy², K. Crocker², M.G. Poirier^{1,2,3}, C. Castro^{1,4}, and R. Bundschuh^{1,2,3,5,6,*}

ABSTRACT In eukaryotic cells, DNA is packaged into chromatin where nucleosomes are the basic packaging unit. Important cellular processes including gene expression, DNA replication, and DNA repair require nucleosomal DNA to be unwrapped so that functional proteins can access their target sites, which otherwise are sterically occluded. A key question in this process is what are the unwrapped conformations individual nucleosomes adopt within chromatin. Here, we develop a concurrent nucleosome unwrapping model to address this question. We hypothesize that for a given end-to-end distance of the nucleosomal DNA, the nucleosomal DNA stochastically unwraps from the histone core from both ends independently and that this combination of unwrapping from both sides results in a significant increase in the average distance between the DNA extending from both sides of the nucleosomes. We test our model on recently published experiments using a DNA origami nanocaliper that quantifies nucleosome unwrapping and achieve good agreement between experiment and model prediction. We then investigate the DNA origami caliper distribution when attached to a hexasome (a nucleosome lacking a H2A/H2B dimer). A significant shift in the caliper angle distribution because of the asymmetric structural features of the hexasome seen experimentally is consistent with the model. Our modeling approach may more broadly be useful to the interpretation of other studies of nucleosome dynamics, chromatin dynamics, and regulatory processes involving nucleosome unwrapping, as well as more generally to optimization of future DNA origami designs to probe mechanical properties of biomolecules.

STATEMENT OF SIGNIFICANCE The genome of eukaryotic cells is compacted to fit into the nucleus by wrapping approximately 147 base pairs of DNA around cores of eight histone proteins each, thereby forming nucleosomes. While this achieves compaction, wrapping of the DNA around the histone protein cores influences and thus regulates cellular processes requiring access to the DNA. It is therefore important to understand the propensity for DNA to temporarily unwrap. The main significance of our work is that we show that if one considers unwrapping from both ends, DNA unwrapping from nucleosomes is 10-100 times more likely than expected from previous quantitative studies of nucleosome unwrapping from individual ends. This implies a less stringent constraint of nucleosome geometry on chromatin structure.

INTRODUCTION

In eukaryotic cells, genomic DNA is packaged into chromatin. The basic packaging unit is the nucleosome, a protein-DNA complex which consists of a histone protein octamer core and approximately 147 base pairs of DNA wrapped around it (1). The nucleosomes interconnect with each other to form a "beads-on-a-string" 10 nm chromatin fiber and higher order chromatin structures (2). Important cellular processes, including DNA transcription, replication, and repair, require transient exposure of nucleosomal DNA to functional DNA binding proteins such as transcription factors, DNA/RNA polymerases, and repair enzymes (3–5). By controlling DNA accessibility within chromatin, nucleosome unwrapping plays

an important role in regulating a number of genetic processes (6–8).

Dynamic DNA unwrapping and rewrapping from an individual histone octamer core has been extensively studied using a number of complementary approaches. Restriction enzyme experiments were first used to quantify transient nucleosome unwrapping (9), while Förster Resonance Energy Transfer (FRET) measurements have been used extensively in both

¹Interdisciplinary Biophysics Graduate Program, The Ohio State University, 484 W. 12th Av., Columbus, OH 43210, USA

²Department of Physics, The Ohio State University, 191 W. Woodruff Av., Columbus, OH 43210, USA

³Department of Chemistry&Biochemistry, The Ohio State University, 100 W, 18th Ay, Columbus, OH 43210, USA

⁴Department of Mechanical Engineering, The Ohio State University, 201 W. 19th Av., Columbus, OH 43210, USA

⁵Division of Hematology, Department of Internal Medicine, The Ohio State University, 320 W. 10th Av., Columbus, OH 43210, USA

⁶Center for RNA Biology, The Ohio State University, 484 W. 12th Av., Columbus, OH 43210, USA

^{*}Correspondence: bundschuh@mps.ohio-state.edu

ensemble and single molecule experiments to quantify both nucleosome unwrapping/rewrapping equilibrium and kinetics (10–15). However, these approaches typically only detect unwrapping from one side of the nucleosome and therefore do not reveal how unwrapping is correlated on the opposite sides of the nucleosome. Single molecule force spectroscopy measurements have been used to induce and detect unwrapping on both sides of single nucleosomes (16) and within nucleosome arrays (17). However, forces applied at opposite ends of a chromatin fiber induce single large unwrapping events corresponding to entire nucleosomes (18, 19) and therefore do not provide information about the continuous and dynamic nature of nucleosome unwrapping. Moreover, the flexible tethers used in these experiments contribute to the force-extension responses, making the force induced extension of individual nucleosomes difficult to measure. Recent single molecule measurements that combine force and FRET allowed for local detection of the force induced unwrapping (20), which revealed that force induced nucleosome unwrapping on one side of the nucleosome suppresses unwrapping on the opposite side. However, the magnitude of this effect was difficult to quantify. Separate restriction enzyme experiments combined with transcription factor binding did not detect this anticorrelation between DNA unwrapping on opposite sides of the nucleosome (21) raising the question of how significant anticorrelated nucleosome unwrapping is. Separate single molecule DNA unzipping experiments provide local information on force induced unwrapping (22), which was used to infer the entire nucleosome unwrapping free energy landscape (23). But again, this only provides information on nucleosome unwrapping/rewrapping on one side of the nucleosome.

A more recent experimental approach uses DNA origami nanocalipers to measure nucleosome unwrapping (24, 25). In these experiments, a single nucleosome is incorporated into a DNA nanocaliper. With the two ends of the nucleosome separately attached to two arms of the caliper, the DNA origami caliper exerts a force on the nucleosome and biases the nucleosome toward more partially unwrapped states that would not be observable on free nucleosomes. The unwrapping process undergoes nanoscale dynamic thermal fluctuations, which results in an unwrapping conformation distribution that is reported by the caliper angle distribution and measured by imaging these conformations with transmission electron microscopy (TEM). This approach is complementary to other methods in that it probes nucleosome unwrapping on both sides of the nucleosome and is sensitive to the continuous nature of nucleosome unwrapping.

Based on this experiment, we developed a concurrent nucleosome unwrapping model to quantitatively describe how individual nucleosomes unwrap/rewrap when constrained at both ends, similar to how they would be within the context of chromatin. In this model, the two ends of the nucleosome can independently unwrap simultaneously, where the length of unwrapped DNA on each side of the nucleosome is individually determined by the interaction between the DNA and the histone core proteins. By comparing the model predictions to the experimental results from Le et al. (24), we find that the presence of multiple unwrapping conformations for a given unwrapping state (end-to-end distance of nucleosome) significantly lowers the free energy cost of unwrapping. These results imply that while unwrapping nucleosomal DNA is a rare event, the additional entropy from a multitude of unwrapping combinations results in a significant increase in the distance between opposite ends of the DNA extending out from the nucleosome, or equivalently in a significantly increased probability to unwrap a given amount of base pairs compared to experiments that probe unwrapping on only one side of the nucleosome at a time as shown in Table 1.

To then further verify our model, we examined replacing the nucleosome within the nanocaliper with a hexasome, which lacks one H2A/H2B dimer. Due to the missing contacts between DNA and the H2A/H2B dimer, a certain length of DNA is expected to always remain unwrapped. We used our model to calculate the caliper angle distribution with varying length of always unwrapped DNA. We then experimentally determined the angle distribution for nanocalipers containing a hexasome and compared it to the calculated caliper angle distribution. We find that our model qualitatively captures the asymmetric structure of the hexasome, further supporting the validity of our concurrent unwrapping model. In combination these results provide insight into how nucleosomes can accommodate constraints on the DNA extending out of the nucleosome and a framework for modeling and designing future nanocaliper experiments studying nucleosomes and other biomolecules.

MATERIALS AND METHODS

Concurrent nucleosome unwrapping model

We consider nucleosomal DNA unwrapping from the histone octamer core and attached to a nanocaliper as shown in Figure 1. We assume that (1) the geometry of nucleosome unwrapping can be described in a two-dimensional plane, (2) the histone octamer has cylindrical shape, 8 nm in diameter, in this plane, and (3) once the dsDNA, 2 nm in cross-section, unwraps from the histone octamer tangentially there is no bending or twisting of the DNA. The latter is a reasonable first assumption because the length of the unwrapped DNA is smaller than the persistence length of DNA ($\sim 50 \, \text{nm}$). However, as we note in the discussion, departure from this assumption might be responsible for remaining deviations between model calculations and experiments. Initially, the DNA is fully wrapped on the histone. We model this case as 147 bp of DNA in contact with the histone octamer for the maximum wrapping of 1.65 times (1) and two extra dsDNA linker segments with variable lengths connected at each end of the positioning sequence. The size of the biotin-neutravidin linkage between the DNA and the DNA origami nanocaliper is taken to be a 5 nm extension beyond the linker DNA. In order

for the positioning sequence to be wrapped 1.65 turns, in our model each bp is taken to be 0.352 nm for the wrapped DNA while 0.34 nm is used for the unwrapped DNA. Note, that this base-pair-step for the wrapped DNA is calculated based on the assumed 10 nm diameter of the mid-point circle of the nucleosomal DNA, which has been used in other nucleosome modeling studies before (26, 27). The geometrical parameters of the model and their values are summarized in Table S1 in the Supporting Material.

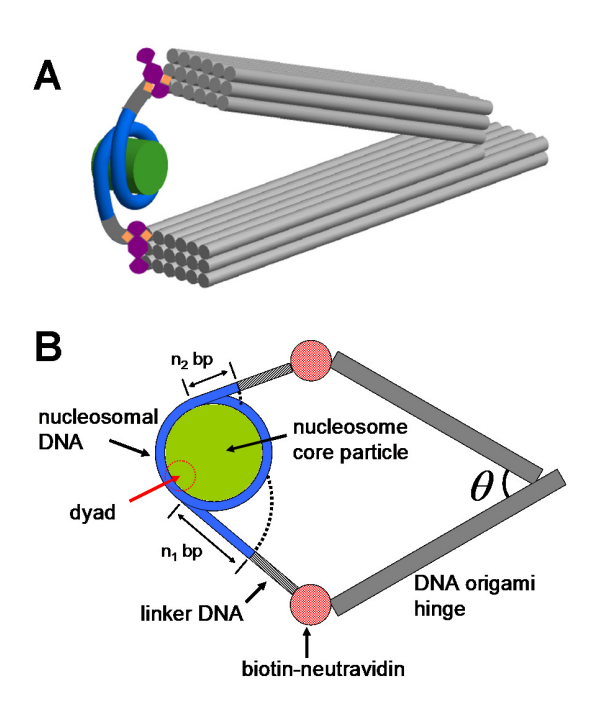


Figure 1: Concurrent nucleosome unwrapping model where a nucleosome is incorporated into a DNA origami nano caliper. (A) 3D structure of the DNA origami caliper-nucleosome system. (B) Geometry of the model. In our DNA origami calipers incorporating nucleosomes experiment, the two ends of a nucleosome are attached to two arms of the caliper, respectively, via linker DNA (additional base pairs of DNA beyond a 147 bp Widom 601 nucleosome positioning sequence at both ends of the nucleosome) and biotin-neutravidin linkages. The caliper acts as a nanoscale torsional spring and applies force on the nucleosome to extend its end-to-end distance. In our model, the two ends of the nucleosome responding to the same external force can unwrap simultaneously and independently, with n_1 bp unwrapped on one side and n_2 bp unwrapped on the other. We use the caliper angle θ as a readout, which can be directly measured on TEM images of the caliper-nucleosome constructs, to report the nucleosome unwrapping state (end-to-end distance). Note that the objects in this figure are for illustration purposes only and do not represent the actual scale of the molecules.

In our nucleosome unwrapping model, the DNA is allowed to be released from the histone octamer core from both sides simultaneously with each side unwrapping independently. This release is associated with a free energy cost $G(n_1, n_2)$ of a given unwrapping state, in which n_1 base pairs are released from the "forward" side and n_2 base pairs are released from the "reverse" side of the nucleosome (here, "forward" and "reverse" are defined based on the Widom 601 nucleosome positioning sequence) (28). The unwrapping free energy $G(n_1, n_2) =$ $G_{\text{forward}}(n_1) + G_{\text{reverse}}(n_2)$ is given by the sum of individual free energy costs from both sides. n_1 and n_2 range from 0 to half of the total length of the positioning sequence (73 bp), which means the DNA in our model cannot be unwrapped beyond the dyad region on the histone core from either side (this is a reasonable approximation since the free energy cost of these larger unwrapping events anyway prevents them from having a significant weight in the calculations).

Caliper angle distribution of DNA origami nanocaliper incorporating a nucleosome

In our DNA origami nanocaliper device, the two ends of the DNA construct that includes nucleosomal and linker DNA are connected to the two nanocaliper arms of length 68 nm through a biotin-neutravidin linkage (24). In the absence of a nucleosome, the DNA origami nanocaliper has an experimentally measured angular distribution $P_{\text{caliper}}(\theta \to \theta + \delta \theta)$, where θ is the nanocaliper angle. In our concurrent unwrapping model, different lengths of nucleosomal DNA can be released from both sides of the histone core simultaneously. Thus, for a given end-to-end distance range from distance d to distance $d + \delta d$ $(d \rightarrow d + \delta d)$ of the nucleosome-linker-construct (measured from one end of the DNA-arm attachment to the other end) or corresponding nanocaliper angle range $\theta \to \theta + \delta\theta$, there are potentially multiple corresponding unwrapping states (n_1, n_2) . The angle distribution $P(\theta \to \theta + \delta \theta)$ of the nanocaliper incorporating a nucleosome can then be calculated as

$$P(\theta \to \theta + \delta\theta) \propto P_{\text{caliper}}(\theta \to \theta + \delta\theta) \times \sum_{(n_1, n_2) \text{ in } \theta \to \theta + \delta\theta} e^{-\frac{G(n_1, n_2)}{k_B T}},$$
(1)

where the summation runs over all possible unwrapping configurations (n_1, n_2) resulting in a nanocaliper angle in the range $\theta \to \theta + \delta\theta$.

This allows numerical calculation of the angle distribution of nanocalipers incorporating nucleosomes. We first set up 6° bins in angle space centered at 0^o , 6^o , For each angle bin, we then enumerate all possible unwrapping configurations (n_1, n_2) which are allowed in this bin and use Equation (1) to calculate the probability of this bin. Due to the steric effect of the biotin-neutravidin linkages which connect the nucleosomal DNA and the DNA origami nanocaliper, we disallow any angles smaller than 4.2° (corresponding to approximately 5 nm biotin-neutravidin linkage size). The final angle distribution of the nanocalipers is obtained by normalizing the probabilities of all angle bins. We performed this calculation for all four DNA linker lengths used in the experiments (6 bp, 26 bp, 51 bp and 75 bp). Error bars for the calculated distributions were obtained by resampling 1000 times from the experimental distribution $P_{\text{caliper}}(\theta \to \theta + \delta \theta)$ of the empty hinge, calculating the standard deviations of the experimental empty hinge distribution in every angle bin from the samples, and multiplying these standard deviations with the same factor as the probability itself is multiplied with in Equation (1). Kolmogorov-Smirnov *P*-values that quantify the probability that the predicted and the experimentally observed distributions are sampled from the same underlying distribution are calculated by scaling the predicted distribution to a total count equal to the total count of the empty hinge experimental distribution used in Equation (1).

Free energy landscapes of nucleosome unwrapping from both ends

Our model described in the previous two sections requires the free energy costs $G_{\text{forward}}(n)$ and $G_{\text{reverse}}(n)$ of unwrapping a specific number n of base pairs from the histone core on one side. The exact values of these free energy costs depend on the DNA sequence and the locations where DNA and histone proteins are in contact. Due to the nonpalindromic nature of the NPS, the unwrapping free energy landscapes from either side of the nucleosome are different (22) $(G_{\text{forward}}(n) \neq G_{\text{backward}}(n))$. The free energy landscape $G_{\text{forward}}(n)$ of unwrapping DNA from the forward direction was previously determined (23) by fitting a quantitative model to the mechanical nucleosome unzipping experiment performed by Wang's group (22). Here, we used the same method to determine the unwrapping free energy landscape $G_{\text{reverse}}(n)$ for unzipping of the opposite side of the nucleosome. Briefly, first we create a trial free energy landscape and, based on this free energy landscape, use the quantitative model in (23) to calculate the expected dwell times of unzipping each DNA base pair. We then vary the trial free energy landscape until we get good agreement (a final Bhattacharyya distance (29) of 0.064) between the calculated dwell times and the experimentally measured dwell times reported in (22).

Preparation of hexasomes

The model presented above indicated that longer linkers should show stronger effects of the hexasome on the caliper angle distributions. Since 75 bp linker constructs failed to efficiently reconstitute hexasomes, we settled for 51 bp linker constructs for hexasome preparation. Biotinylated DNA molecules containing the Widom 601 NPS with Gal4 binding site (CCGGAGGCTGCCCTCCGG) at the 8th – 26th base pairs consistent with previously published work (24) were prepared by PCR using oligonucleotides containing a biotin label on the 5'-end (Table S2 in the Supporting Material) for integration into the nanocaliper. DNA molecules were purified by phenol-chloroform extraction and then purified by anion-exchange HPLC using a Gen-Pak Fax column (Waters). Recombinant X. laevis histones H2A(K119C), H2B, H3(C110A) and H4 were expressed, purified and refolded into H3/H4 tetramers and H2A/H2B dimers separately for use in hexasome preparation. The H2A(K119C)/H2B(WT) dimers were labeled with Cy5-maleimide (GE Healthcare) and purified as detailed in a previous publication (30). Hexasomes were reconstituted with the double salt dialysis method by mixing purified histone tetramer, histone dimer, and DNA previously used to reconstitute nucleosomes (31). The recovered nucleosomes were then analyzed by Electrophoretic Mobility Shift Assay (EMSA). Hexasome reconstitution was optimized by first titrating the amount of dimer against fixed tetramer and DNA concentration (x:1:1.3) until well formed hexasomes were observed before proceeding to purification. For purification, hexasomes were loaded into 5-30% sucrose gradients made with 0.5x TE and purified by ultracentrifugation (Beckman Coulter, Optima L-90K) at 4 °C, 41,000 rpm for 22 h in a SW41 rotor. The gradient was analyzed by 5% polyacrylamide native gel electrophoresis after ultracentrifugation, and fractions containing hexasomes without tetrasomes or nucleosomes (the three highest mobility species) were collected and concentrated. Neutravidin was added to purified hexasomes at a 10:1 molar ratio and fractions containing hexasomes with two neutravidins were purified by ultracentrifugation with a 5-30% sucrose gradient as described above. Figure S1 in the Supporting Material shows TEM images of purified hexasomes.

Preparation of DNA origami nanocalipers

The DNA origami nanocaliper design is comprised of 2 bundles of 18 double-stranded DNA connected together by 6 single-stranded DNA connections as previously reported in (24, 32). 184 unique DNA oligonucleotides were thermally annealed to an 8,064 nucleotide ssDNA scaffold derived from M13mp18 plasmid variant in an annealing ramp with a 15 minute melt time at 65°C, a 4 hour annealing time at 52°C, and a 15 minute cool time at 4°C. Structures were folded in 18 mM MgCl₂, 5mM Tris, 5mM NaCl, and 1mM EDTA buffer conditions to form a DNA origami nanocaliper. The structures were characterized by gel electrophoresis and transmission electron microscopy (TEM) as previously described (24, 33). For hexasome experiments, the structures were purified via centrifugation with protocols modified from (34). 15% PEG8000 (Sigma Life Science) diluted in 200mM NaCl were combined in equivolumes of unpurified structures. The combined solution was centrifuged at 16,000g for 30 minutes to pellet structures. After PEG-based centrifugal purification, nanocalipers were resuspended to 8 nM in 59 mM Tris, 1.7 mM MgCl₂, 240 mM NaCl, pH 8.0.

Preparation of hexasome-caliper assemblies

Hexasome samples were diluted to 5 nM in 0.5x TE pH 8.0 after sucrose gradient purification. Then, 1 μ l of the 7.5 nM

calipers was combined with $1 \mu l$ of the 5 nM nucleosomes and an additional $2 \mu l$ of a 63.5 mM Tris, 1.0 mM MgCl₂ and 260 mM NaCl solution for an equimolar final concentration 1 nM:1 nM (nanocalipers : hexasomes) in a final buffer of 50 mM Tris, 1 mM MgCl₂, and 200 mM NaCl. We previously confirmed the stability of the nanocalipers in the buffer over the timescale of our measurements (Figure S18 in (24)). The mixed solution was incubated on ice for 30 minutes and then immediately deposited on the TEM grid. Figure S2 in the Supporting Material shows sample TEM images.

TEM imaging

Sample imaging and analysis by TEM are done as in (24). Hexasome-nanocaliper assemblies were deposited and incubated for 4 minutes onto Formvar-coated copper grids (Electron Microscopy Services). The sample was wicked off and the copper grids were stained with 2% uranyl formate (SPI, West Chester, PA) and immediately wicked off. The copper grid was dabbed gently with filter paper until all residual liquid was taken off and allowed to dry for at least 15 minutes. TEM was carried out at the Ohio State University Campus Microscopy and Imaging Facility, located at OSU, on a FEI Tecnai G2 Spirit TEM. Samples were imaged at an acceleration voltage of 80kV at a magnification of 85,000x. A combination of Mathematica, ImageJ, and eman2 was used to quantify the conformation of the samples as previously described in (24). Caliper angle measurements were obtained manually via Image J's angle measurement tools along the inner edges of the caliper arms.

Caliper angle distribution of DNA origami nanocaliper incorporating a hexasome

Hexasome-nanocaliper assemblies were modeled analogously to nucleosome-nanocaliper assemblies described above. However, in order to account for the missing copy of the H2A/H2B dimer, we only allow states with arbitrary n_1 but $n_2 \ge n$, where we vary *n* from 0 to 60 in order to identify its optimal value. We only restrict n_2 since hexasomes have been shown (35) to incorporate into the Widom 601 NPS with the dimer missing at the reverse side.

RESULTS

Quantitative modeling of nucleosome unwrapping in the context of DNA origami nanocalipers

We base our model and calculation on the DNA origami nanocaliper developed by Le et al. (24). In this caliper, the two ends of a nucleosome are attached to the two arms of the caliper as shown in Figure 1A. In order to develop a model we first identify the relevant degrees of freedom of the system. Based on the design of the system, its variable regions are the base of the caliper, the flexible connections between the

caliper arms and the nucleosome, and the unwrapping of the DNA off the nucleosome. We model all other aspects of the structure as rigid. The most complicated of the variable regions is the unwrapping of the nucleosome since there are two ends of the DNA that can unwrap to different extents. Similar to (36) we describe this unwrapping in terms of two variables n_1 and n_2 that quantify the number of base pairs unwrapped on either end of the nucleosome as shown in Figure 1B. Once the amount of unwrapping from both sides is fixed, the experimental observable, namely the caliper angle θ , is determined by geometry. We then describe the interaction between the DNA and the histone core by free energy landscapes of unwrapping DNA from either end of the nucleosome. In order to fully include all nonlinearities of the mechanical behavior of the free nanocaliper in the model we use the measured angle distribution of a nanocaliper without nucleosomes to characterize the intrinsic angle preferences of the nanocaliper. Using partition function theory, we can then calculate the caliper angle distribution in the presence of nucleosomes and compare it to experiment. More details on the model are given in the methods section.

The free energy landscape of unwrapping nucleosome differs between two sides

A main ingredient to modeling the nucleosome-nanocaliper assemblies, but also more generally to quantitatively understanding any experiment involving nucleosome unwrapping, is the unwrapping free energy landscape. The free energy landscape of nucleosome unwrapping describes the free energy cost associated with unwrapping each DNA base pair from the histone core particle. The detailed interactions between the histone core particle and DNA have been characterized by an experiment carried out by Wang's group (22) where the nucleosomal DNA is mechanically unzipped from the histone core particle. In this experiment, it was found that the free energy landscapes of the two sides of the nucleosome differ from each other due to the sequence difference between the two sides of the Widom 601 NPS. We will refer to one side of the nucleosome as the "forward" side (strong interaction, red DNA in Figure 2A) and the other side as the "reverse" side (weak interaction, blue DNA in Figure 2A). Previously, Forties et al. (23) determined the free energy landscape for unwrapping the forward side by fitting a trial free energy landscape to the mechanical unzipping experiment (Figure 2B). Since nucleosomes in the experiments we are modeling here can unwrap from both sides, we need to know the unwrapping free energy landscape of the reverse side as well. Thus, we use the same method as Forties et al. (23) to determine this free energy landscape of the reverse side. Briefly, we first assume a trial free energy landscape and then calculate the corresponding reverse side dwell time distribution based on the trial free energy landscape. We compare the calculated distribution to the dwell time distribution observed in the mechanical unzipping experiment. We then vary the trial free energy landscape and iterate this process until the corresponding dwell time distribution is in good agreement with experimental observations (Figure 2C). We find a Bhattacharyya distance (29) of 0.064 between the experimental dwell time distribution and the dwell time distribution derived from the optimized free energy landscape. The Bhattacharyya distance between two distributions measures their similarity and is zero if they are equal and infinity if the two distributions do not have any overlap. Figure 2D compares the forward and reverse unwrapping free energy landscapes with each other. We find that they are overall very similar, which might at first be somewhat surprising given the large differences in the measured dwell time distributions but becomes clear when realizing that changes in the free energy landscape have an exponential influence on dwell times. The most significant differences are in the 35-45 bp region, where the reverse landscape is lacking the strong rise (indicating especially strong DNA histone interactions) in the forward landscape, and in the dyad region. We note that in the dyad region both free energy landscapes rise a lot faster past the central (73rd) nucleotide than before the central nucleotide. This might at first sight appear as a contradiction as unwrapping just past the central nucleotide in one of the landscapes involves breaking the same DNA-histone contacts as unwrapping just before the central nucleotide in the opposite landscape. However, unwrapping just before the central nucleotide occurs in the vicinity of the still wrapped opposite end of the nucleosomal DNA while for unwrapping past the central nucleotide the neighboring DNA strand is not present leading to a much stronger electrostatic attraction between the DNA and the histone core to be overcome during unwrapping in that regime.

Comparison model and experiments confirms the concurrent unwrapping model

We tested our concurrent nucleosome unwrapping model on the recently published experiments by Le et al. (24) where nucleosomes are incorporated into DNA origami nanocalipers. In these experiments, the nucleosomes are reconstituted using canonical histone octamer and the Widom 601 NPS. The DNA linkers on these nucleosomes are of equal distances with possible lengths of 6, 26, 51, and 75bp denoted as 6L, 26L, 51L, and 75L, respectively. The ends of the DNA linkers are then attached to the arms of the nanocaliper via a biotin-neutravidin linkage to create a nucleosome-nanocaliper assembly. More than 200 of such structures are measured in TEM images to create an angular distribution (solid gray bars, Figure 3). These angular distributions reflect the balance between the nucleosomes' tendency to remain wrapped and the nanocalipers' tendency to remain open. Both of these tendencies are included in our model and the goal of this study is to disentangle the two by comparison between experimental data and model predictions. To this end, we calculate the angle distribution of nucleosome-nanocaliper assemblies with different DNA linker lengths (green open bars, Figure 3A)

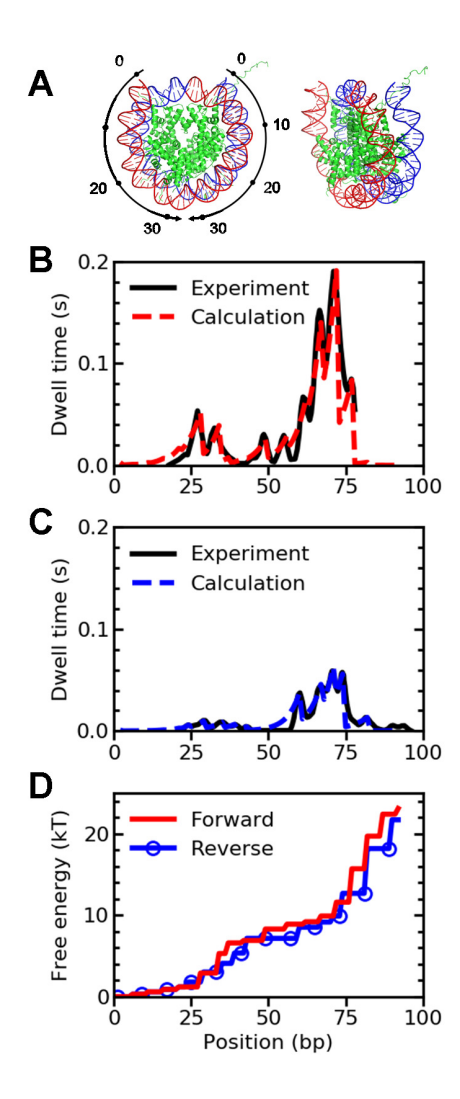


Figure 2: Nucleosome unwrapping from both sides. (A) Left: Crystal structure of the nucleosome (PDB ID: 1AOI (1)). Axes indicate the number of bp along nucleosomal DNA. Red: forward side of DNA. Blue: reverse side of DNA. Right: side view of the nucleosome. (B) Experimental (solid) and calculated (dashed) dwell time distribution for forward unwrapping (from (23)). (C) Experimental (solid) and calculated (dashed) dwell time distribution for reverse unwrapping. In both (B) and (C) the experimental dwell time distributions are from mechanical unzipping experiments by the Wang group (22). (D) Free energy landscape (FEL) for unwrapping the '601' positioning DNA sequence from a nucleosome core particle. Red: forward unwrapping FEL. Blue: reverse unwrapping FEL. The FELs in (D) are derived by fitting the calculated dwell times to the experiment.

based on our model without any adjustable parameters. In order to quantify the agreement between calculated and experimentally determined angle distributions, we calculate the Bhattacharyya distance (29) between the predicted and the experimental angle distribution (denoted d in Figure 3).

We find that, the predictions agree reasonably well with the experiment for all different linker lengths. For 6L, 26L, 51L, and 75L, the Bhattacharyya distances between prediction and experiment are 0.11 ± 0.01 , 0.09 ± 0.01 , 0.07 ± 0.01 , and 0.04 ± 0.01 , respectively, where the error bars were determined by resampling 1000 times with replacement from the experimental distribution. Kolmogorov-Smirnov P-values quantifying the probability that the experimental and the theoretical distributions are sampled from the same distribution are $1.27 \cdot 10^{-18}$, $1.69 \cdot 10^{-12}$, $2.38 \cdot 10^{-7}$, and $1.89 \cdot 10^{-4}$ for the four linker lengths, respectively. This reflects the fact that the Kolmogorov-Smirnov P-value is overly stringent since it focuses only on counting error and not other sources of sample-to-sample fluctuations but also indicates that there are still aspects of the nucleosome-nanocaliper system that our model may be missing as further elaborated on in the discussion section.

An important aspect of our model is that both sides of the nucleosome are allowed to unwrap concurrently. The question if the two sides of a nucleosome can unwrap concurrently or not and if this behavior is intrinsic or depends on the application of an external force has recently been hotly debated in the field (20, 21, 37, 38). Thus, we wanted to contrast our concurrent unwrapping model with variants that do not allow independent unwrapping on both sides of the nucleosome. The key in a non-concurrent model, no matter if one limits unwrapping to only one side of the nucleosome, allows unwrapping of only one side at a time, or chooses some other mechanism to avoid concurrent unwrapping, is that in contrast to the concurrent model the number of unwrapping configurations does not increase with the total number of unwrapped base pairs. To be specific, we chose two among the several different ways one could implement a non-concurrent model: (i) the one where either side of the nucleosome can unwrap but if one of the sides unwraps, the other must remain wrapped (namely $n_1n_2 = 0$), which we term the single-sided model, and (ii) the one where the length of DNA unwrapped from one side of the nucleosome is equal to the length of DNA unwrapped from the other side (namely $n_1 = n_2$), which we term the symmetric model. We again compare the calculated angle distributions to the experimental distributions (Figures 3B and C). The Bhattacharyya distances between calculated and experimental angle distributions for 6L, 26L, 51L and 75L are 0.33 ± 0.03 , 0.37 ± 0.03 , 0.37 ± 0.04 , and 0.30 ± 0.03 for the single-sided and 0.10 ± 0.01 , 0.09 ± 0.01 , 0.11 ± 0.02 , and 0.13 ± 0.02 for the symmetric model, respectively. Comparing these distances, the corresponding Kolmogorov-Smirnov P-values, and the visual appearances of the distributions with the concurrent model, the concurrent model clearly yields a better description of the experimental results for all linker lengths. The symmetric model performs similarly to the concurrent model for the short linker lengths but becomes clearly less consistent with the experimental data for the longer linker lengths. This result supports our conclusion that in the nanocaliper experiments the nucleosome adopts multiple possible conformations at a

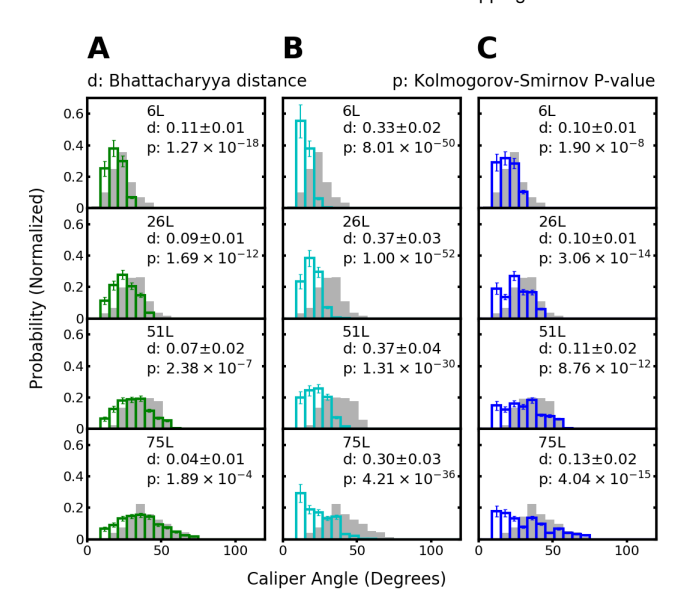
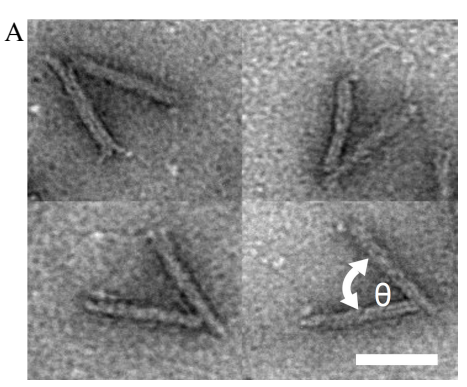


Figure 3: Comparison between concurrent, single-sided, and symmetric model predictions. (A) The comparison between the concurrent unwrapping model prediction and experiment; Column (B) (middle): the comparison between the singlesided unwrapping model prediction and experiment; (C) The comparison between the symmetric unwrapping model prediction and the same experiment. Gray: caliper distributions measured from calipers incorporating nucleosomes experiments; blue and green: calculated caliper distributions. 6L, 26L, 51L and 75L are the lengths of the DNA linkers (in number of base pairs) attached to both ends of the nucleosome. Error bars on the predicted distributions are calculated by resampling from the free hinge distribution as described in the Methods section. d is the Bhattacharyya distance (29) between the experimental and predicted caliper distributions. The standard error on d is obtained by resampling the experimental data with replacement. 'p' is the Kolmogorov-Smirnov P-value quantifying the probability that the experimental and predicted caliper distributions are drawn from the same underlying distribution.

given end-to-end distance (or corresponding caliper angle) rather than only one or a few, as it would in a non-concurrent scenario.

Hexasomes have significantly larger end-to-end distances than nucleosomes

To demonstrate the generalizability of our concurrent model, we performed similar experiments using the nanocaliper to investigate unwrapping as Le et al. (24), but with hexasomes instead of nucleosomes. To this end, we have prepared hexasomes, consisting of one tetramer and one heterodimer, using the Widom 601 sequence with a 51 bp DNA linker extending from both sides (51L hexasomes) attached to both arms of the nanocaliper via a biotin-neutravidin linkage. The hexasome-nanocaliper assembly has $\approx 50\%$ efficiency in joining both arms of a hexasome construct to both arms of a single nanocaliper (Figure 4A).



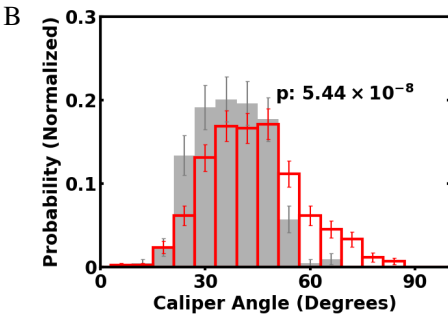


Figure 4: DNA origami nanocalipers incorporating hexasomes with 51 bp DNA linkers. The hexasomes were reconstituted using the Widom 601 positioning sequence with 51 bp DNA linker at both ends. (A) Transmission electron microscopy images of calipers incorporating hexasomes. θ is the caliper angle. Scale bars = 50 nm. (B) Experimental angle distribution of nanocalipers incorporating hexasomes (red) and angle distribution of nanocalipers with nucleosomes from the experiments in (24) (gray). Error bars are determined by resampling 1000 times from the experimental distributions with replacement and calculating the standard deviation of the counts in every angle bin from these random samples. 'p' is the Kolmogorov-Smirnov P-value quantifying the probability that the two experimental distributions are drawn from the same underlying distribution.

We measure the conformation of 420 hexasome-nano-caliper assemblies in the TEM. The angular distribution of the 51L hexasomes has a mean angle of 43.9° with a range from 6.4° to 84.8°. In contrast, the distribution of the 51L nucleosomes has a mean of 36.6° and a range of 0° to 69.4° (Figure 4B). The Kolmogorov-Smirnov P-value quantifying the probability that the two experimental distributions are sampled from the same underlying distribution is a highly significant $1.04 \cdot 10^{-25}$. Thus, the 51L hexasomes-nanocaliper assemblies have an angle distribution favoring significantly larger angles than that of the 51L nucleosome-nanocaliper assemblies, indicating that hexasome constructs favor states

that are more unwrapped than their nucleosomal counterparts, consistent with the loss of DNA-histone contacts on one side.

The concurrent unwrapping model captures the asymmetric structure of hexasome unwrapping.

We postulate that the main difference between the unwrapping behavior of a hexasome and the unwrapping behavior of a nucleosome is the lack of an opportunity for beneficial interactions between the DNA and the histone core at the site of the missing H2A/H2B dimer. Thus, there is no reason for the DNA to remain wrapped at the end where the contacts with the H2A/H2B dimer have been eliminated and indeed cryo-EM structures of hexasomes support the picture of the DNA that would be bound by the H2A/H2B dimer in the nucleosome protruding straight out of the hexasome (38). This suggests a simple modification of our model to describe the hexasome experiments: we exclude configurations where the DNA on the side of the hexasome with the missing dimer is not sufficiently unwrapped. Formally, we define a minimum number n of base pairs that must remain permanently unwrapped on the side of the hexasome with the missing dimer, i.e., we only allow configurations with arbitrary (n_1, n_2) but limited to $n_2 \ge n$ and leave all other aspects of the model unchanged. Since we do not know a priori how many base pairs remain unwrapped due to the missing dimer, we vary the length n of permanently unwrapped DNA and compare the caliper angle distribution predicted by the resulting model for a large range of possible lengths n of permanently unwrapped DNA in Figure 5 to the experimental observation shown as the red open bars in Figure 4. Among calculations with *n* ranging from 0 bp to 60 bp, the best agreement is obtained for n = 20 bp based on the Bhattacharyya distance (0.07 ± 0.01) and for n = 25 based on the Kolmogorov-Smirnov *P*-value $(1.71 \cdot 10^{-3})$. These levels of agreement are similar to or better than the agreement we obtained for nucleosomes with the same linker length, which further verifies our model and demonstrates the capability of our model to capture the asymmetric structural features of hexasomes.

DISCUSSION

In summary, we studied the mechanism by which single nucleosomes undergo conformational changes when the DNA is attached at both ends of the nucleosome. This configuration is important since it corresponds to the natural chromatin context: when a nucleosome has to fit into a particular chromatin geometry it does not depend on the probability that one particular side of the nucleosome unwraps, but instead depends on the probability that the two ends of the nucleosome span the particular distance required by the geometric context. We proposed a detailed mathematical model in which each single nucleosome undergoes stochastic and often asymmetric unwrapping fluctuations and adopts multiple possible unwrap-

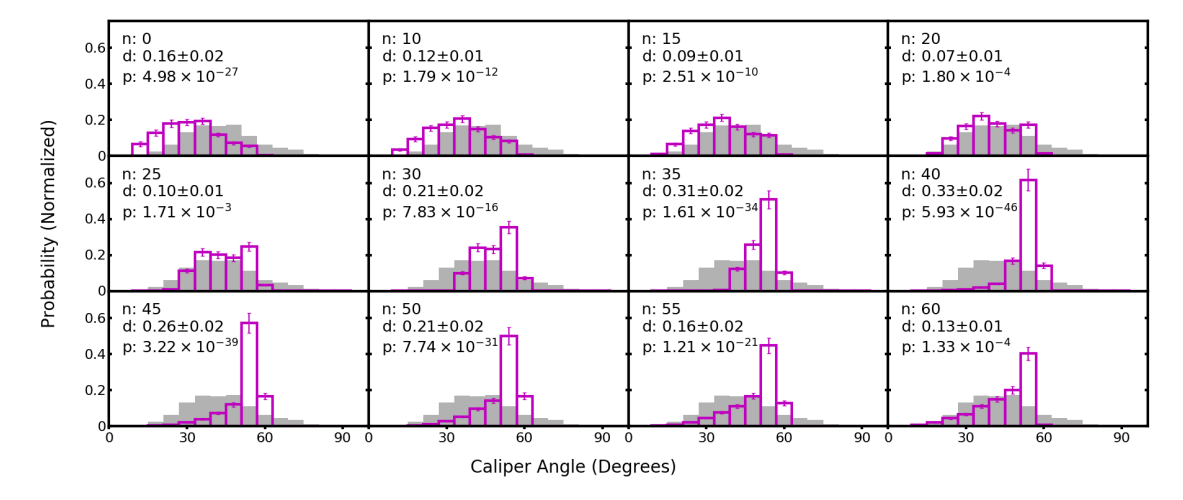


Figure 5: Comparison between model prediction and experimental distribution of hexasomes incorporated into DNA origami calipers. Hexasomes in this experiment have 51L DNA linkers. In our model for hexasomes, we assumed a certain length of DNA (in number of bp) to be always unwrapped on the side where the H2A/H2B dimer is missing. We calculated the caliper angle distributions incorporating hexasomes with varying lengths of unwrapped DNA and compare them to the experimental measurement shown as the red open bars in Figure 4. Subfigures are comparisons of angle distributions between the caliper-hexasome experiment (identical in all subfigures) and trial caliper-hexasome calculations with varying length of exposed DNA. Solid gray: experimental caliper distribution with hexasomes; open purple: predicted caliper distribution with hexasome, n on the upper right of each figure indicates the minimum length of DNA unwrapped in the calculation. Error bars on the predicted distributions are calculated by resampling from the free hinge distribution as described in the Methods section; error bars for the experimental distribution are omitted for the sake of clarity but can be found in Figure 4. d is the Bhattacharyya distance (29) between the experimental and the calculated distribution. The standard error on d is obtained by resampling the experimental data with replacement. 'p' is the Kolmogorov-Smirnov P-value quantifying the probability that the experimental and predicted caliper distributions are drawn from the same underlying distribution.

ping configurations at a given unwrapping state (end-to-end distance). We confirmed our model by comparing the model predictions to recent experiments on nucleosome-nanocaliper assemblies (24). We note that a similar DNA origami device probing nucleosomes as the one modeled here was developed by Funke et al. (25). The latter was used to explore the salt induced nucleosome disassembly. Since the histone-DNA interaction depends on the salt conditions, our model calculations cannot be directly compared to the Funke et al. experiment, which were carried out at higher MgCl₂ concentrations. In addition to comparing to the experiments by Le et al. (24), we conducted an independent experiment on hexasome-nanocaliper assemblies to verify the predictive capability of our model.

A significant contribution of our work is highlighting a mechanism that promotes unwrapping in situations where the ends of the nucleosome are fixed. In previous experimental and theoretical studies on nucleosome unwrapping, the emphasis is usually on individual unwrapping from one side of the nucleosome (10, 11). This results in unwrapping being considered a relatively rare event suppressed by free energy costs on the order of several k_BT . E.g., based on the free energy landscape known before this study, i.e., the forward side of the Widom 601 NPS alone, it is estimated that un-

wrapping events of 20, 30, and 40bp occur with probabilities of $2.1 \cdot 10^{-2}$, $3.3 \cdot 10^{-3}$, and $6.0 \cdot 10^{-5}$, respectively (see Table 1). The newly determined free energy landscape for the weaker reverse side of the Widom 601 NPS only somewhat modifies those to $1.9 \cdot 10^{-2}$, $3.1 \cdot 10^{-3}$, and $3.0 \cdot 10^{-4}$. Compared to unwrapping from one side, our concurrent nucleosome unwrapping model accommodates a multitude of possible configurations at a given end-to-end distance (or corresponding caliper angle as measured in the DNA origami experiments) decreasing the free energy cost for unwrapping to a certain end-to-end distance by introducing additional entropy. For a rough estimate of this entropic contribution we can for simplicity assume that the end-to-end distance depends only on the total number n of unwrapped base pairs and that all n + 1 combinations of n_1 and n_2 with $n = n_1 + n_2$ have the same unwrapping free energy $G(n_1, n_2)$. This would lead to an entropy boost of $k_B \ln(n + 1)$ or a free energy decrease of $3 - 4k_BT$ for 20-40 total unwrapped base pairs. For the Widom 601 NPS taking all the geometric details of the model and the unwrapping free energies $G(n_1, n_2)$ into account the full calculation yields probabilities of $3.2 \cdot 10^{-2}$, $2.2 \cdot 10^{-2}$, and $8.8 \cdot 10^{-3}$ for 20, 30, and 40 total unwrapped base pairs, respectively, which are significantly higher than the probabilities one obtains when looking at one side alone. By contrasting with predictions of non-concurrent models, we show that the concurrent aspect of our model is crucial to explaining the relatively frequent unwrapping observed in the DNA origami caliper experiments (24). This implies that concurrent unwrapping plays a similar role in increasing the frequency of unwrapping compared to asymmetric unwrapping in the context, where neighboring nucleosomes as part of chromatin structure instead of an artificial DNA origami device define the end-to-end distance of the nucleosome.

Table 1: Probabilities to unwrap 20, 30, and 40 base pairs from the forward side of the nucleosome alone, from the reverse side of the nucleosome alone, and concurrently. It can be seen that the additional entropy of the concurrent unwrapping significantly increases the unwrapping probabilities for the larger numbers of unwrapped base pairs.

bp unwrapped	forward only	reverse only	both sides
20	$2.1 \cdot 10^{-2}$	$1.9 \cdot 10^{-2}$	$3.2 \cdot 10^{-2}$
30	$3.3 \cdot 10^{-3}$	$3.1\cdot 10^{-3}$	$2.2\cdot 10^{-2}$
40	$6.0 \cdot 10^{-5}$	$3.0 \cdot 10^{-4}$	$8.8 \cdot 10^{-3}$

The concurrent aspect of our model is also consistent with direct measurements of DNA extensions. If nucleosomes unwrapped only on one side at a time, hexasomes, which are naturally unwrapped at the side where the heterodimer is missing, should not unwrap at all at the opposite side. We therefore traced the DNA contours in all 37 hexasome images, in which the DNA was actually visible including 13, in which the DNA was visible on both sides of the hexasome (unfortunately the staining of the TEM images allows only a small fraction of the DNA molecules to be traced). Figure S3 in the Supporting Material shows some representative images, the histogram of all 50 quantified DNA lengths, and a scatter plot of the two lengths measured for the 13 images, in which both sides of the DNA were visible. If hexasomes unwrapped only on the side on which the heterodimer is missing, the shorter of the two DNA lengths should be 51 nucleotides or 17 nm for all 13 images, while the longer of the two DNA lengths is fluctuating. This expectation is clearly not consistent with the data with only one point being close to 17 nm. On the contrary, the points in Figure S3B are broadly scattered, further supporting our concurrent unwrapping model.

Importantly, while the experiments and thus also our model use the 601 nucleosome positioning sequence, the general effect that entropic contributions from asymmetric unwrapping increase the probability of unwrapping should be independent of DNA sequence. For a different sequence we would expect that the respective "forward only" and "reverse only" unwrapping probabilities are different than their 601 counterparts used here but that asymmetric unwrapping still leads to a similarly increased probability for unwrapping from both sides as the entropic gain of a few k_BT estimated above is independent of DNA sequence. Thus, while the comparison between experiment and modeling that revealed the importance of this entropic gain has been performed for the 601 sequence, the mechanism should be relevant for arbitrary genomic sequences.

It is essential to note that even the entropically enhanced unwrapping probabilities in the lower single digit percent range would hardly be observable, were it not for the DNA origami nanocaliper exerting a force on the nucleosome. Figure S4 in the Supporting Material illustrates this point by showing the probability distributions of the number of unwrapped bases corresponding to the angle distributions in Figure 3A predicted by our model. While a free nucleosome is expected to be mostly fully wrapped with unwrapping probabilities to 20 bp in the single digit percent as discussed above, the probability of these states is in the 20%-25% range when attached to the nanocaliper. Still, the fully wrapped states $(\leq 4 \text{ bp unwrapped})$ are observed with probabilities of 0.008, 0.026, and 0.04 for the linker lengths of 26, 51, and 75bp, respectively (for a linker length of 6bp, our assumed geometry actually forbids these nearly fully wrapped states) even in the presence of the nanocalipers and are thus probed relatively to the unwrapped states that the nanocalipers emphasize.

These findings are in agreement with other force spectroscopy studies on nucleosome unwrapping. It was reported in a previous paper (32), which used the same nanocaliper as our study, that the nanocaliper applies a torque of 35 pN nm at the smallest angle of 20° explored in that study. The free nanocaliper distribution from Le et al. (24) used as input to our model shows the largest change in probability from an opening angle of 0^o to an opening angle of 6^o and this change constitutes a factor of 7.3. This corresponds to a torque of 80 ± 40 pN nm, where the uncertainty stems from the relatively low counts in the empirical probability distribution for these small angles. Since the DNA extending out from the nucleosomes is attached to the nanocaliper arms, which are 68 nm in length from the hinge vertex, the force applied at the ends of the arms is at most 1-2 pN. A number of studies have reported that in this force range, the outer portion of the nucleosomal DNA partially unwraps (16, 20, 39). In fact, the magnetic tweezers measurements from the van Noort lab (39) report that at a force of 2.5 pN, the outer turn of the nucleosome has a probability of 0.5 to be unwrapped. Therefore, in our nanocaliper measurements, since the force range applied by the nanocaliper is 0 to 2 pN, both the fully wrapped and partially unwrapped states of the nucleosome are populated.

A second important contribution of this work is the determination of the unwrapping free energy landscape for the "reverse" side of the Widom 601 NPS. While models based on DNA mechanics have characterized sequence dependent differences in nucleosome stability and unwrapping (37, 40, 41), the reverse side free energy landscape presented here is directly derived from experimental data and thus includes contributions from DNA conformational changes as well as from any rearrangements of the histone core due to unwrapping. Its

comparison with the forward free energy landscape shows an overall similar profile but important differences of a few k_BT in the region of contact with the H2A/H2B dimer and in the dyad region. We hope that this will spur more experimental investigations into the sequence dependence of the unwrapping free energy landscape.

Our model agrees reasonably well with experimentally observed DNA origami caliper angle distributions incorporating nucleosomes and qualitatively reproduces the experimental observations on hexasomes incorporated into DNA origami calipers as well. However, there are still statistically significant deviations between our model and nucleosome experiments, only some of which are likely due to the fact that the Kolmogorov-Smirnov statistics ignores the uncertainties inherited by the predicted distributions from the underlying experimental free hinge distribution, especially in cases of short linkers where the peak of the predicted distribution is in an angle range that is weakly sampled in the experimental free hinge distribution. In addition, one aspect of our model's prediction on hexasomes does not quantitatively agree with geometric analysis and existing experiments such as enzymatic digestion studies on hexasomes (42, 43). Both indicate that the length of unwrapped DNA due to the missing H2A/H2B dimer should be around 40 bp; however, our model yields best agreement if the number of unwrapped base pairs is in the range of 20 to 25.

One possible reason for the discrepancies could be bending of the DNA, which we have excluded in our model. In order to quantify the amount of bending of the DNA in our hexasome experiments, we used the 50 traced DNA contours from the 37 images used in Figure S3 and averaged the cosines of the angle differences as a function of contour length (Figure S5 in the Supporting Material). For a worm-like chain, this quantity should exhibit an exponential decay with the slope indicating the persistence length. The persistence length of DNA under physiological conditions is known to be 50 nm and the somewhat elevated magnesium concentrations in our experiments should lead to even shorter persistence lengths (44). Yet, the fit in Figure S5 yields a persistence length of 65 nm \pm 14 nm and even a fit that ignores the short distance effects and focuses on contour lengths of 4 nm and higher yields a persistence length of around 56 nm. We thus conclude that the DNA in our experiments does not undergo any excessive bending beyond what is expected based on its intrinsic flexibility. Also, bending of the DNA would, if anything, cause the nanocalipers to exhibit smaller angles. Hence, accounting for bending in the models would increase the discrepancy with the experimental data and further exclude the non-concurrent models for nucleosome unwrapping. However, as quantified in Figure S5 the bending that we observe is slight, and would likely cause only minor changes in observed angles.

Another possible reason for the discrepancies is that our assumption of complete independence between the unwrapping on both sides is oversimplified. While we have conclusively shown that a model that allows unwrapping only on one side at

a time is not consistent with the data, it is possible that unwrapping on one side does affect unwrapping on the other, i.e., that our assumption $G(n_1, n_2) = G_{\text{forward}}(n_1) + G_{\text{reverse}}(n_2)$ is not strictly true. In fact, this assumption must become incorrect as $n_1 + n_2 \gtrsim 85$ due to the electrostatic interaction between the neighboring DNA gyres, even though unwrapping events of this magnitude do not seem to play a role in the experiments modeled here.

Further, discrepancies between the experiments and the model could be due to different buffer conditions between the experiments by the Wang group (22), from which the free energy landscapes are extracted, and the DNA origami experiments in Le et al. (24). The experiments from the Wang group (22) were done in a buffer with 100 mM Na⁺, and 0.5 mM free Mg²⁺, while the DNA origami experiments (24) were performed in 200 mM Na⁺ and 1 mM Mg²⁺ to maintain stability of the DNA origami. While in general buffer conditions can play a large role in the stability of nucleosomes, recent single molecule FRET studies show that there is minimal impact on nucleosome unwrapping in this particular range of sodium concentrations (45). The increase in free Mg²⁺ concentration from 0.5 mM to 1 mM also should play only a minor role (10) and if anything will stabilize the nucleosome (46) and thus lead to more wrapped nucleosomes and smaller caliper opening angles; the deviations between our model predictions and the experimental angle distributions go in the opposite direction. We thus conclude that salt effects are not likely candidates for explaining the remaining discrepancies between model and experiment. We also note that our main conclusion that the amount of unwrapping in the DNA origami experiment is surprisingly high when compared to unwrapping from one side at a time, is even more so true given that the buffer conditions in the DNA origami experiments if anything should suppress unwrapping. Lastly, the discrepancies could be due to the fact that the model we proposed is limited to two dimensions, which may not adequately describe the actual nucleosome and hexasome structures in three dimensional space. However, a three dimensional treatment would require detailed information on the free energy landscape of unwrapping the DNA in all possible spatial directions and is thus beyond the scope of the discussion of this paper.

We also notice that the DNA origami caliper angle distribution predicted by our model is less accurate for shorter DNA linkers than longer DNA linkers, especially for 6L and 26L. The predicted angle distribution is visually smaller than the experimental distribution. This is likely due to the steric interactions between the DNA origami device, neutravidin, and the nucleosome when they get very close to each other. These interactions are not fully taken into account in our model and are subject of future extensions of the model.

A notable feature of the calculated angle distributions is their apparent "ruggedness", which one might expect of an experimentally determined but not of an analytically calculated distribution. One reason for this ruggedness is that the calculation does take the experimental angle distribution of

the free caliper as input. However, a more important reason for the ruggedness is the strong variation of accessible states from angle bin to angle bin. To illustrate this point, Figure S6 in the Supporting Material shows the number of configurations per angle bin, both for the concurrent and the symmetric unwrapping model. To understand the variability, we categorize these unwrapping configurations into four different modes: mode 1 (blue), in which there is at least one turn of DNA wrapped around the histone core and the two ends of the DNA cross over; mode 2 (green), in which there is at least one turn of DNA wrapped around the histone core and the two ends of the DNA do not cross over; mode 3 (purple), in which there is less than one turn of DNA wrapped around the histone core and the two ends of the DNA cross over; and mode 4 (yellow), in which there is less than one turn of DNA wrapped around the histone core and the two ends of DNA do not cross over. These data indicate that one major discontinuity is due to the disappearance of modes 2 and 3. For the symmetric model, the overall smaller number of states generates additional fluctuations due to the discrete nature of the binning by angle.

CONCLUSION

Through development of a quantitative theoretical model, comparison of this model with previous experiments on nanocalipers containing nucleosomes, and follow-up experiments on nanocalipers containing hexasomes, we have identified concurrent unwrapping as a mechanism that significantly lowers the barrier to nucleosome unwrapping compared to what is observed when studying unwrapping of one side of the nucleosome alone. Since nucleosomes are attached at both ends in their natural chromatin context, the lowered barriers to unwrapping found here are important when interpreting the amount of nucleosome unwrapping in the natural chromatin context. In the future, we believe that our model, validated by experiments, can be used to guide the design of other calipers with different mechanical properties (i.e. free caliper angle distribution, torsional stiffness, etc) to probe other aspects of nucleosome mechanics and chromatin structure, and also assist in expanding the current usage of calipers to the study of other biological complexes.

AUTHOR CONTRIBUTIONS

RB, CC, and MGP designed the research. DZ and KC performed the quantitative modeling, MAD prepared hexasomes, and JVL prepared the nanocalipers and performed TEM experiments on them. All authors contributed to the writing of and approved the final manuscript.

ACKNOWLEDGMENTS

We would like to thank the Campus Microscopy and Imaging Facility at The Ohio State University. This material is based upon work supported by the National Science Foundation under Grants No. DMR-1410172, DMR-1719316, and MCB-1715321.

REFERENCES

- 1. Luger, K., A. W. Mader, R. K. Richmond, D. F. Sargent, and T. J. Richmond, 1997. Crystal structure of the nucleosome core particle at 2.8 A resolution. Nature 389:251-260.
- 2. Kornberg, R. D., 1974. Chromatin structure: a repeating unit of histones and DNA. Science 184:868-871.
- 3. Li, B., M. Carey, and J. L. Workman, 2007. The role of chromatin during transcription. Cell 128:707-719.
- 4. Almouzni, G., and H. Cedar, 2016. Maintenance of Epigenetic Information. Cold Spring Harbor perspectives in biology 8:a019372.
- 5. Sinha, M., and C. L. Peterson, 2009. Chromatin dynamics during repair of chromosomal DNA double-strand breaks. *Epigenomics* 1:371–385.
- 6. North, J. A., J. C. Shimko, S. Javaid, A. M. Mooney, M. A. Shoffner, S. D. Rose, R. Bundschuh, R. Fishel, J. J. Ottesen, and M. G. Poirier, 2012. Regulation of the nucleosome unwrapping rate controls DNA accessibility. Nucleic acids research 40:10215-10227.
- 7. Workman, J. L., and R. E. Kingston, 1998. Alteration of nucleosome structure as a mechanism of transcriptional regulation. Annual review of biochemistry 67:545-579.
- 8. Hodges, C., L. Bintu, L. Lubkowska, M. Kashlev, and C. Bustamante, 2009. Nucleosomal fluctuations govern the transcription dynamics of RNA polymerase II. Science 325:626-628.
- 9. Polach, K. J., and J. Widom, 1995. Mechanism of protein access to specific DNA sequences in chromatin: a dynamic equilibrium model for gene regulation. Journal of molecular biology 254:130-149.
- 10. Li, G., and J. Widom, 2004. Nucleosomes facilitate their own invasion. Nature structural & molecular biology 11:763-769.
- 11. Li, G., M. Levitus, C. Bustamante, and J. Widom, 2005. Rapid spontaneous accessibility of nucleosomal DNA. Nature structural & molecular biology 12:46-53.
- 12. Kelbauskas, L., N. Woodbury, and D. Lohr, 2009. DNA sequence-dependent variation in nucleosome structure, stability, and dynamics detected by a FRET-based analysis. Biochem. Cell Biol. 87:323-335.

- 13. Koopmans, W. J., R. Buning, T. Schmidt, and J. van Noort, 2009. spFRET using alternating excitation and FCS reveals progressive DNA unwrapping in nucleosomes. Biophys. J. 97:195-204.
- 14. Andresen, K., I. Jimenez-Useche, S. C. Howell, C. Yuan, and X. Qiu, 2013. Solution scattering and FRET studies on nucleosomes reveal DNA unwrapping effects of H3 and H4 tail removal. PLoS ONE 8:e78587.
- 15. Luo, Y., J. A. North, and M. G. Poirier, 2014. Single molecule fluorescence methodologies for investigating transcription factor binding kinetics to nucleosomes and DNA. Methods 70:108-118.
- 16. Mihardja, S., A. J. Spakowitz, Y. Zhang, and C. Bustamante, 2006. Effect of force on mononucleosomal dynamics. Proc. Natl. Acad. Sci. U.S.A. 103:15871-15876.
- 17. Brower-Toland, B. D., C. L. Smith, R. C. Yeh, J. T. Lis, C. L. Peterson, and M. D. Wang, 2002. Mechanical disruption of individual nucleosomes reveals a reversible multistage release of DNA. Proc. Natl. Acad. Sci. U.S.A. 99:1960-1965.
- 18. Cui, Y., and C. Bustamante, 2000. Pulling a single chromatin fiber reveals the forces that maintain its higherorder structure. Proc. Natl. Acad. Sci. U.S.A. 97:127-132.
- 19. Bennink, M. L., S. H. Leuba, G. H. Leno, J. Zlatanova, B. G. de Grooth, and J. Greve, 2001. Unfolding individual nucleosomes by stretching single chromatin fibers with optical tweezers. Nat. Struct. Biol. 8:606-610.
- 20. Ngo, T. T. M., Q. Zhang, R. Zhou, J. G. Yodh, and T. Ha, 2015. Asymmetric unwrapping of nucleosomes under tension directed by DNA local flexibility. Cell 160:1135-1144.
- 21. Moyle-Heyrman, G., H. S. Tims, and J. Widom, 2011. Structural constraints in collaborative competition of transcription factors against the nucleosome. J. Mol. Biol. 412:634-646.
- 22. Hall, M. A., A. Shundrovsky, L. Bai, R. M. Fulbright, J. T. Lis, and M. D. Wang, 2009. High-resolution dynamic mapping of histone-DNA interactions in a nucleosome. *Nature structural & molecular biology* 16:124–129.
- 23. Forties, R. A., J. A. North, S. Javaid, O. P. Tabbaa, R. Fishel, M. G. Poirier, and R. Bundschuh, 2011. A quantitative model of nucleosome dynamics. Nucleic acids research 39:8306-8313.
- 24. Le, J. V., Y. Luo, M. A. Darcy, C. R. Lucas, M. F. Goodwin, M. G. Poirier, and C. E. Castro, 2016. Probing Nucleosome Stability with a DNA Origami Nanocaliper. ACS nano 10:7073-7084.

- 25. Funke, J. J., P. Ketterer, C. Lieleg, P. Korber, and H. Dietz, 2016. Exploring Nucleosome Unwrapping Using DNA Origami. Nano letters 16:7891-7898.
- 26. Kunze, K. K., and R. R. Netz, 2002. Complexes of semiflexible polyelectrolytes and charged spheres as models for salt-modulated nucleosomal structures. Phys. Rev. E 66:011918.
- 27. Dobrovolskaia, I. V., and G. Arya, 2012. Dynamics of forced nucleosome unraveling and role of nonuniform histone-DNA interactions. Biophys. J. 103:989-998.
- 28. Lowary, P. T., and J. Widom, 1998. New DNA sequence rules for high affinity binding to histone octamer and sequence-directed nucleosome positioning. J. Mol. Biol. 276:19-42.
- 29. Kailath, T., 1967. The Divergence and Bhattacharyya Distance Measures in Signal Selection. IEEE Transactions on Communication Technology 15:52-60.
- 30. Shimko, J. C., J. A. North, A. N. Bruns, M. G. Poirier, and J. J. Ottesen, 2011. Preparation of fully synthetic histone H3 reveals that acetyl-lysine 56 facilitates protein binding within nucleosomes. J. Mol. Biol. 408:187-204.
- 31. Luger, K., T. J. Rechsteiner, and T. J. Richmond, 1999. Expression and purification of recombinant histones and nucleosome reconstitution. Methods Mol. Biol. 119:1-16.
- 32. Marras, A. E., L. Zhou, H. J. Su, and C. E. Castro, 2015. Programmable motion of DNA origami mechanisms. Proc. Natl. Acad. Sci. U.S.A. 112:713-718.
- 33. Castro, C. E., F. Kilchherr, D. N. Kim, E. L. Shiao, T. Wauer, P. Wortmann, M. Bathe, and H. Dietz, 2011. A primer to scaffolded DNA origami. Nat. Methods 8:221-229.
- 34. Stahl, E., T. G. Martin, F. Praetorius, and H. Dietz, 2014. Facile and scalable preparation of pure and dense DNA origami solutions. Angew. Chem. Int. Ed. Engl. 53:12735-12740.
- 35. Levendosky, R. F., A. Sabantsev, S. Deindl, and G. D. Bowman, 2016. The Chd1 chromatin remodeler shifts hexasomes unidirectionally. Elife 5:e21356.
- 36. Teif, V. B., R. Ettig, and K. Rippe, 2010. A lattice model for transcription factor access to nucleosomal DNA. Biophys. J. 99:2597-2607.
- 37. de Bruin, L., M. Tompitak, B. Eslami-Mossallam, and H. Schiessel, 2016. Why Do Nucleosomes Unwrap Asymmetrically? J. Phys. Chem. B 120:5855–5863. PMID: 26991771.

- 38. Bilokapic, S., M. Strauss, and M. Halic, 2018. Histone octamer rearranges to adapt to DNA unwrapping. Nat. Struct. Mol. Biol. 25:101-108.
- 39. Kruithof, M., and J. van Noort, 2009. Hidden Markov analysis of nucleosome unwrapping under force. Biophys. J. 96:3708-3715.
- 40. Tolstorukov, M. Y., A. V. Colasanti, D. M. McCandlish, W. K. Olson, and V. B. Zhurkin, 2007. A novel rolland-slide mechanism of DNA folding in chromatin: implications for nucleosome positioning. J. Mol. Biol. 371:725-738.
- 41. Becker, N. B., and R. Everaers, 2009. DNA nanomechanics in the nucleosome. Structure 17:579-589.
- 42. Arimura, Y., H. Tachiwana, T. Oda, M. Sato, and H. Kurumizaka, 2012. Structural analysis of the hexasome, lacking one histone H2A/H2B dimer from the conventional nucleosome. Biochemistry 51:3302–3309.
- 43. Rychkov, G. N., A. V. Ilatovskiy, I. B. Nazarov, A. V. Shvetsov, D. V. Lebedev, A. Y. Konev, V. V. Isaev-Ivanov, and A. V. Onufriev, 2017. Partially Assembled Nucleosome Structures at Atomic Detail. *Biophys. J.* 112:460– 472.
- 44. Brunet, A., C. Tardin, L. Salomé, P. Rousseau, N. Destainville, and M. Manghi, 2015. Dependence of DNA Persistence Length on Ionic Strength of Solutions with Monovalent and Divalent Salts: A Joint Theory-Experiment Study. Macromolecules 48:3641–3652.
- 45. Gansen, A., S. Felekyan, R. Kuhnemuth, K. Lehmann, K. Toth, C. A. M. Seidel, and J. Langowski, 2018. High precision FRET studies reveal reversible transitions in nucleosomes between microseconds and minutes. Nat Commun 9:4628.
- 46. Yang, Z., and J. J. Hayes, 2011. The divalent cations Ca2+ and Mg2+ play specific roles in stabilizing histone-DNA interactions within nucleosomes that are partially redundant with the core histone tail domains. Biochemistry 50:9973-9981.

SUPPLEMENTARY MATERIAL

An online supplement to this article can be found by visiting BJ Online at http://www.biophysj.org.